Journal of
Cardiovascular Development and Disease

MDPI

Article

Plasma Lipocalin-2 and Echocardiographic Indices After Isolated Right Pulmonary Artery Ligation in Rats: Associations with Right Ventricular Systolic Pressure and Histologic Remodeling

Jiao Yang, Ning Ma *, Hongju Zhang, Ruijuan Su, Li Xue, Liyuan Xu and Yan Sun

Department of Echocardiography, Cardiac Center, National Center for Children's Health, Beijing Children's Hospital, Capital Medical University, Beijing 100045, China; yang_jiaode@163.com (J.Y.); hjzhang73@126.com (H.Z.); sulon1015@163.com (R.S.); 15801602757@163.com (L.X.); xuliyuanyx@163.com (L.X.); sunxiaoyan01@sina.com (Y.S.)
* Correspondence: maning_echo@163.com; Tel.: +86-133-7011-1551

Abstract

Isolated right pulmonary artery ligation redirects flow to the contralateral lung. We tested whether adding plasma lipocalin-2 (LCN2) to echocardiography improves discrimination between ligation and sham operation. Male Sprague–Dawley rats undergoing ligation or sham operation ($n = 16$ each) were assessed at postoperative weeks 4, 8, or 12 by echocardiography, right-heart catheterization, histology, and LCN2 immunoassay. Leave-one-out ridge-logistic regression compared echocardiographic models with and without LCN2. The models distinguish ligation from sham and do not grade pulmonary hypertension. At week 4, LCN2, right ventricular systolic pressure, medial wall thickness percentage, and collagen volume fraction differed between groups; echocardiographic indices did not differ significantly. This is between-group separation in different animals, not earlier detection within one animal. The area under the curve (AUC) was 0.914 (95% confidence interval [CI] 0.798–0.992) without LCN2 and 0.945 (0.847–1.000) with LCN2, a nonsignificant increase (ΔAUC +0.031; 95% CI 0.000–0.089; $p = 0.174$). The supported increments were in integrated discrimination (0.061; 95% CI 0.031–0.095) and continuous prediction of right ventricular systolic pressure (leave-one-out R^2 0.819 to 0.847). The in-sample nested change in R^2 was 0.028 (95% CI 0.0008–0.087; false-discovery-rate q = 0.004). These internal results establish neither residual severity grading nor replacement of right-heart catheterization.

Keywords: lipocalin-2; right pulmonary artery ligation; volume-overload pulmonary hypertension; echocardiography

Check for updates

Academic Editor: Christos G. Mihos

Received: 8 October 2026
Revised: 28 October 2026
Accepted: 4 November 2026
Published: 6 November 2026

Copyright: © 2026 by the authors. Licensee MDPI, Basel, Switzerland. This article is an open access article distributed under the terms and conditions of the Creative Commons Attribution (CC BY) license.

1. Introduction

Pulmonary hypertension (PH) secondary to congenital heart disease (CHD-PH) often begins as reversible volume overload from left-to-right shunts and may progress to fixed vascular remodeling, motivating serial noninvasive phenotyping in the early hyperperfusion window [1–5]. Right-heart catheterization (RHC) remains the hemodynamic reference for diagnosis and severity grading. However, ionizing radiation exposure, procedural risk, and high technical demands limit its suitability for frequent repetition. These constraints are particularly relevant in children, in whom cumulative radiation, anesthesia exposure, and vascular access considerations further restrict serial invasive surveillance [2,3]. Therefore, echocardiography is used first-line for longitudinal assessment, but concordance with invasive pressure can be limited early after volume overload, owing to suboptimal acoustic

windows, inter-operator variability, and the indirect nature of Doppler-derived pressure surrogates [2,3,6,7]. This early discordance is clinically consequential: the hyperperfusion window is precisely when intervention may still modify disease trajectory. Conventional imaging alone may fail to capture the evolving right ventricular pressure load and vascular remodeling. Circulating remodeling biomarkers may complement imaging when repeated catheterization is impractical, offering an accessible, repeatable source of pathophysiologic information that could enhance the interpretive yield of routine echocardiography.

Lipocalin-2 (LCN2; also known as neutrophil gelatinase-associated lipocalin [NGAL]) is a secreted glycoprotein involved in inflammation, iron homeostasis, and tissue remodeling. It has been extensively studied in oncology as a biomarker and mediator linked to tumor-cell survival, proliferation, and progression [8]. Pulmonary arterial smooth-muscle cell hyperproliferation and apoptosis resistance in PH share features with neoplastic remodeling, providing a biologic rationale for examining oncology-related effectors such as LCN2 in this context [9]. Clinical observational studies have reported a link between elevated circulating LCN2 level and PH [10,11]. Experimental studies have shown pro-remodeling effects of LCN2 on pulmonary arterial smooth-muscle cells [12–14]. However, toxin-/drug-induced experimental paradigms cause chemical vasculopathy and systemic toxicity and poorly recapitulate early high-flow volume overload of shunt-associated CHD-PH [4,5]. Isolated right pulmonary artery ligation (RPAL) redirects flow to impose exclusive left-lung volume overload, approximating early hyperperfusion physiology while avoiding toxin-based injury [15]. The phenotype reported for this ligation is higher right ventricular systolic pressure together with increased medial wall thickness and increased myocardial collagen [15]. In this paper, "experimental volume-overload PH" refers to that phenotype. It does not mean a clinical diagnosis of pulmonary hypertension, and it does not mean established irreversible pulmonary vascular disease. Whether circulating LCN2 level rises in experimental volume-overload PH and whether plasma LCN2 provides incremental information to an echocardiographic panel against catheter and histopathologic reference endpoints remain incompletely defined.

Using this RPAL rat model, we aimed to (1) characterize circulating LCN2 during early pulmonary hyperperfusion and its associations with right ventricular systolic pressure and histologic remodeling, and (2) evaluate whether adding plasma LCN2 to echocardiography improves discrimination between ligation and sham operation within this early window. These aims were pursued as an internal, hypothesis-generating analysis and were not intended to replace RHC.

2. Materials and Methods

2.1. Ethics and Reporting

All procedures in this study were conducted following institutional guidelines and the Guide for the Care and Use of Laboratory Animals [16]. The study was approved by the Institutional Animal Care and Use Committee of MDL Biotech (MDL2026-03-09-07). The study is reported following ARRIVE 2.0 [17].

2.2. Animals and Study Design

Nine-week-old male Sprague–Dawley rats (baseline body weight, approximately 294–339 g; MDL Biotech, Beijing, China) were acclimated for 7 days. Only male rats were used because estrogen can modulate inflammatory responses and iron metabolism, and fluctuations associated with the estrous cycle could introduce hormonal variability into these pathways. Male rats were therefore selected to minimize hormonal confounding in this initial investigation of circulating LCN2. The rats were randomly allocated, using a computer-generated randomization sequence, to the RPAL or sham operation (SO) group,

with terminal assessment at weeks 4, 8, or 12 under specific pathogen-free housing conditions (23 ± 1 °C; 50–60% humidity; 12-h:12-h light–dark cycle). No formal sample-size calculation was performed for the incremental area under the curve (AUC). Approximately 7–8 rats per group were planned for analysis at each terminal week, on grounds of feasibility and by reference to a prior right pulmonary artery ligation model [15]. Enrollment was 7 or 8 animals per cell (group × terminal week; Table 1). The plan did not add animals to offset deaths. After deaths, 5–6 animals per cell were analyzed. This sample can describe group differences and internal cross-validated prediction. It is too small for a precise estimate of a small change in the area under the curve. This sample does not support a claim that the models are stable or generalizable. Subcutaneous hydrochlorothiazide, 25 mg/kg once daily for seven postoperative days, was administered as edema prophylaxis under the protocol common to both operations. That protocol did not specify different doses for ligation and sham operation. Injection logs were not retained, so identical administration cannot be confirmed animal by animal. Fluid balance, electrolytes, and renal function were not monitored. Perioperative analgesia was induced following institutional protocols. Predefined exclusions included severe wound infection, complete hemothorax, large pleural effusion, incomplete ligation, failed catheterization, and anesthetic nonrecovery. Of 45 operated rats, 13 died (28.9%); the remaining 32 with complete multimodal data were analyzed (SO, 16; RPAL, 16; Table 1).

Table 1. ARRIVE-oriented animal flow: enrollment, deaths by planned terminal week, proximate causes, and final analyzed *n*.

Group	Planned Week	Enrolled	Deaths	Final *n*	Cause of Death (*n*)
RPAL	4	8	3	5	Wound infection at 1 week (1); ventricular fibrillation after ultrasound anesthesia, failure to recover (1); intraoperative aortic injury with massive hemorrhage (1)
RPAL	8	8	3	5	Thoracic hemorrhage on postoperative day 1 (1); acute pulmonary embolism after ligation (1); death during right-heart catheterization (1)
RPAL	12	8	2	6	Death during echocardiography (1); acute pulmonary embolism after ligation (1)
RPAL	Subtotal	24	8	16	Attrition 33.3% (8/24)
SO	4	7	2	5	Wound infection on postoperative day 3 (1); intraoperative hemorrhage (1)
SO	8	7	1	6	Failure to recover from anesthesia/surgery (1)
SO	12	7	2	5	Postoperative pneumothorax (1); death during right-heart catheterization (1)
SO	Subtotal	21	5	16	Attrition 23.8% (5/21)
All	Total	45	13	32	Overall mortality 28.9% (13/45)

RPAL, right pulmonary artery ligation; SO, sham operation. Attrition = deaths/enrolled. Final $n = 32$ (SO 16; RPAL 16). Animals that died were excluded from every endpoint. No baseline comparison between animals that died and animals that were analyzed was available.

2.3. Surgical Procedures

Operations were performed under inhaled isoflurane (3% induction; 1.5–2.0% maintenance) with mechanical ventilation (tidal volume, 10 mL/kg; rate, 70 breaths/min; FiO_2, 21%). A right thoracotomy through the third or fourth intercostal space exposed the right pulmonary artery between the superior vena cava and right main bronchus. The RPAL group underwent complete ligation with 9-0 polypropylene suture to impose left-lung volume overload (ligation-only RPALG arm of Meng et al., without a cervical shunt) [15].

The SO group underwent identical dissection without ligation. After air evacuation and layered closure, the rats were weaned from ventilation and recovered on a warming pad.

2.4. Transthoracic Echocardiography

At the assigned terminal week, rats were anesthetized with inhaled isoflurane (3% induction; 1.5–2.0% maintenance) for echocardiography. Imaging was performed using a Vevo 2100 system with an MS250 21-MHz transducer (VisualSonics, Toronto, ON, Canada). Indices averaged over three consecutive stable cycles included right ventricular diameter (RVD)1, RVD2, right ventricular outflow tract diameter (RVOTD), right ventricular wall thickness (RVWT), pulmonary artery diameter (PAD), tricuspid annular plane systolic excursion (TAPSE), pulmonary artery peak velocity (PAV), pulmonary artery ejection time (ET), pulmonary artery acceleration time (AT), and AT/ET [2,7]. Exploratory TAPSE/(AT/ET) and TAPSE × AT (mm·ms) were computed as pulmonary artery systolic pressure (PASP)-independent constructs when tricuspid regurgitation (TR) was inadequate for guideline-based TAPSE/PASP; neither was treated as equivalent to pressure–volume-validated TAPSE/PASP [18,19]. Acquisition and offline analysis were blinded to group.

2.5. RHC

Immediately after echocardiography, the rats were maintained under isoflurane anesthesia, orotracheally intubated, and mechanically ventilated. A 2F high-fidelity micromanometer-tipped catheter (TM-BL420S; 1 kHz sampling) was advanced via the right external jugular vein under waveform guidance. The catheter was positioned in the right ventricle and was not advanced into the right ventricular outflow tract or the pulmonary artery. After ≥30 s of stable intraventricular tracings, right ventricular systolic pressure (RVSP) was recorded by a blinded investigator [2,6].

2.6. Plasma LCN2 Enzyme-Linked Immunosorbent Assay (ELISA)

Blood was collected at the terminal session, after echocardiography and immediately after right-heart catheterization, under the same isoflurane anesthesia. About 5 mL was drawn from the cardiac cavity. Plasma was separated at 3000 rpm (1000× g) for 10 min at 4 °C. LCN2 was measured with a rat lipocalin-2/NGAL ELISA (JYM0044Ra; stated range 0.156–10 ng/mL). On the day of the assay, the kit was equilibrated at room temperature for 30 min. Each sample well received 50 µL of plasma and 50 µL of biotin-antigen working solution. The plate was incubated at 37 °C for 30 min, washed five times, incubated with 50 µL of avidin–horseradish peroxidase at 37 °C for 30 min, and washed five times again. Color reagents A and B (50 µL each) were added, and color was developed for 10 min at 37 °C, protected from light. The reaction was stopped with 50 µL of stop solution. Absorbance was read at 450 nm within 10 min, using the blank well as zero. The LCN2 assay was performed blinded to experimental group.

2.7. Histopathology and Morphometry

Because RPAL elevates load in the left pulmonary circulation, vascular morphometry focused on the left lung. After phosphate-buffered saline (PBS) perfusion, the left lower lobe was formalin-inflated and fixed for 24 h. Elastic–van Gieson (EVG)-stained sections were used for arteriolar morphometry (external diameter [ED] < 200 µm): medial wall thickness percentage (%MT) = (ED − ID) × 100/ED, where ID is the internal diameter. The right ventricular hypertrophy index (RVHI) was calculated using the Fulton index (RV/[LV + septum]) [20]. Myocardial collagen volume fraction (CVF) was quantified on Masson's trichrome sections using ImageJ 1.54f under blinded conditions.

2.8. Statistical Analysis

Statistical analyses were performed using Python 3.12 (SciPy, statsmodels, scikit-learn). The study design was cross-sectional (distinct animals at weeks 4, 8, and 12). Pooled and week-stratified SO versus RPAL comparisons were performed using Mann–Whitney *U* tests for RVSP, RVHI, %MT, CVF, LCN2, and the full echocardiographic panel (including TAPSE/[AT/ET] and TAPSE × AT). Spearman correlations were used to assess predictor–endpoint associations ($n = 32$).

Primary Track 1 used ridge-logistic leave-one-out cross-validation (LOOCV).

$$\text{M1} = \text{RVD1} + \text{PAD} + \text{PAV} + \text{AT/ET} + \text{postoperative week.}$$

$$\text{M2} = \text{M1} + \text{plasma LCN2.}$$

The four echocardiographic indices in M1 were the strongest correlates of right ventricular systolic pressure in this sample. Secondary exploratory tracks (Tracks 2 and 3) were E1–E2 (TAPSE/(AT/ET) ± LCN2) and E3–E4 (TAPSE × AT ± LCN2). These constructs are not equivalent to TAPSE/PASP [18,19].

The ridge penalty was fixed at C = 1.0 before model comparison. Standardization parameters were estimated inside each leave-one-out training fold and applied to the held-out animal. Bootstrap 95% confidence intervals (CIs) were obtained by resampling the paired leave-one-out predicted probabilities (B = 2000) [21]. For a difference in area under the curve, the interval is the 2.5th and 97.5th percentiles of that paired distribution, rounded to three decimals, and the *p* value is the two-sided tail probability from the same resamples. The rounded interval is not an inversion of the *p* value. With a discrete area under the curve, the 2.5th percentile can sit on zero while that tail probability remains above 0.05. Youden cutoffs were derived from the full sample after model fitting. Standardized full-sample ridge-logistic coefficients are reported in Table S1. The negative coefficients for postoperative week are not interpreted as week effects.

Spearman partial correlations of LCN2 with the reference endpoints were estimated by residualizing ranks and then correlating the residuals, with percentile bootstrap 95% confidence intervals from 5000 resamples. Ranks were residualized on terminal-week indicators, and separately on terminal-week indicators and surgical group. Correlations were also estimated within the ligated animals and within the sham-operated animals, with and without residualizing on week.

Metrics assessed were the leave-one-out area under the curve, integrated discrimination improvement based on leave-one-out probabilities [22], and leave-one-out ridge prediction of right ventricular systolic pressure and, secondarily, the hypertrophy index, medial wall thickness percentage, and collagen volume fraction, with Bland–Altman analysis for M2 [23] and calibration of the M2 predictions. The continuous models used a ridge penalty of $\alpha = 1.0$. That α is not the logistic penalty C. The nested ordinary-least-squares change in R^2 from M1 to M2 used Benjamini–Hochberg false-discovery-rate control across four endpoints (Table S2). Sensitivity analyses included full-panel ridge models, with and without LCN2, at C = 0.1, and unpenalized M1 and M2. Two-sided $p < 0.05$ denoted significance.

3. Results

3.1. Study Sample and Attrition

Forty-five rats underwent surgery, and 13 died (28.9%), leaving 32 animals for analysis (ligation, 16; sham, 16; 5–6 per cell; Table 1). Mortality was 33.3% (8/24) after ligation and 23.8% (5/21) after sham operation. The cause and timing of each death are listed by planned terminal week in Table 1. The deaths include intraoperative events, deaths in the first postoperative week, and deaths during terminal echocardiography or catheterization.

3.2. Hemodynamics and Remodeling Endpoints

Week-stratified Mann–Whitney comparisons showed higher RVSP in the RPAL group than in the SO group at week 4 (median 31.6 vs. 26.3 mmHg; $p = 0.008$), week 8 (34.3 vs. 27.05 mmHg; $p = 0.008$), and week 12 (37.1 vs. 26.5 mmHg; $p = 0.008$) (Table S3, Figure 1). %MT, CVF, and plasma LCN2 level were already higher at week 4, with broader between-group separation in remodeling measures at weeks 8–12 (Table S3).

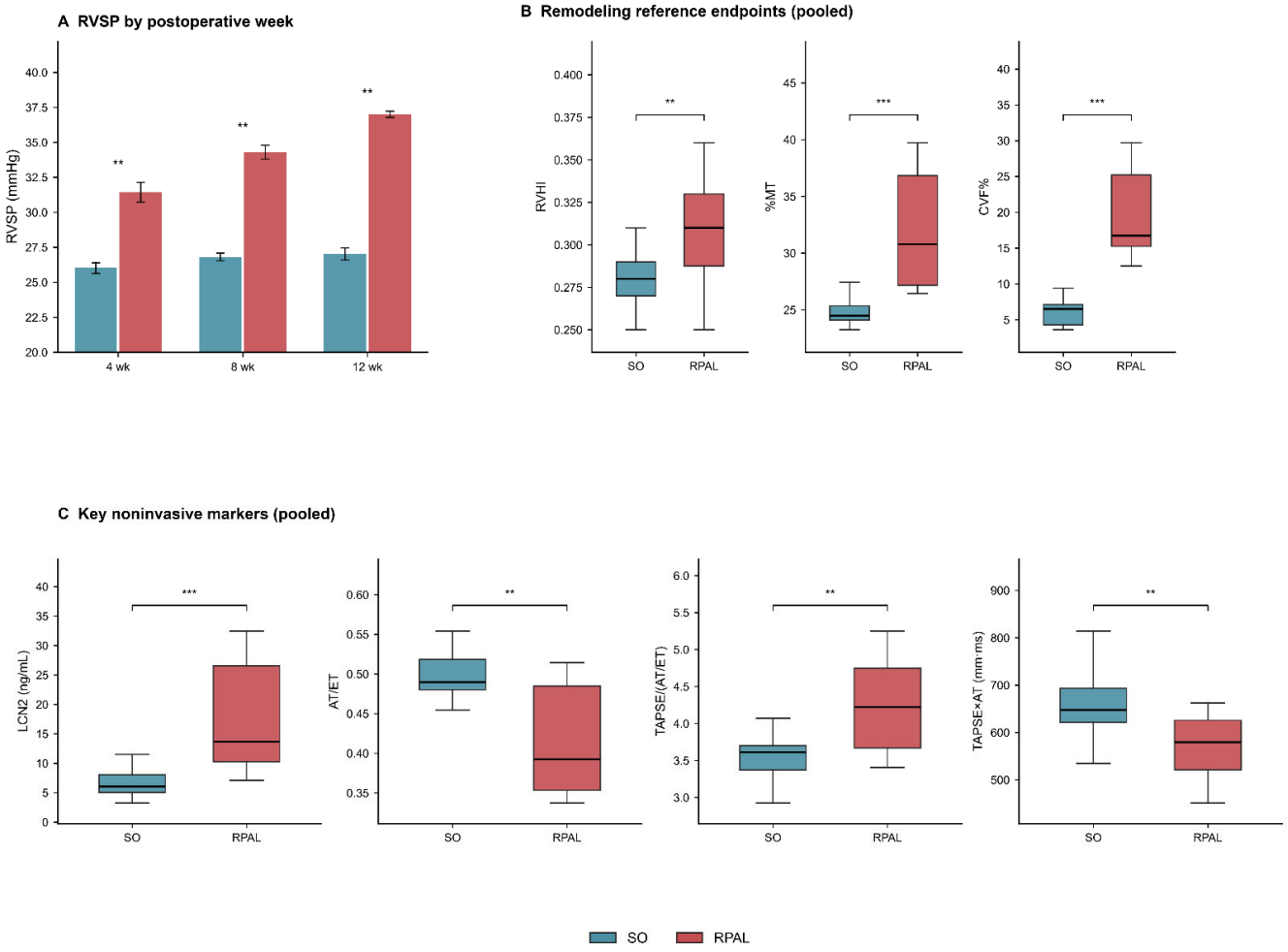


Figure 1. Right ventricular systolic pressure, the hypertrophy index, and remodeling after right pulmonary artery ligation. (**A**) Right ventricular systolic pressure as mean ± standard error of the mean at postoperative weeks 4, 8, and 12. (**B**) Pooled hypertrophy index, medial wall thickness percentage, and collagen volume fraction. (**C**) Pooled lipocalin-2, AT/ET, TAPSE/(AT/ET), and TAPSE × AT. Panels (**B**,**C**) are box plots (median, interquartile range, and range). Blue, sham operation; red, right pulmonary artery ligation. Each terminal week in panel A included 5–6 animals per group. Pooled panels used 16 animals per group. Asterisks in (**A**) indicate within-week two-sided Mann–Whitney *U* tests. Asterisks in (**B**,**C**) indicate pooled two-sided Mann–Whitney *U* tests. ** $p < 0.01$; *** $p < 0.001$. The lipocalin-2 panel includes values above the stated upper calibrator of 10 ng/mL; those values were not diluted. RVSP, right ventricular systolic pressure; RVHI, right ventricular hypertrophy index; %MT, medial wall thickness percentage; CVF, collagen volume fraction; LCN2, lipocalin-2; AT, pulmonary artery acceleration time; ET, pulmonary artery ejection time; TAPSE, tricuspid annular plane systolic excursion.

Pooled across weeks, RVSP (34.60 vs. 26.55 mmHg; $p < 0.001$), RVHI (0.31 vs. 0.28; $p = 0.006$), %MT (30.78% vs. 24.48%; $p < 0.001$), and CVF (16.75% vs. 6.50%; $p < 0.001$) of the RPAL group were higher than those of the SO group (Table 2). The Hodges–Lehmann estimate of the ligation-minus-sham difference was 8.05 mmHg for right ventricular systolic

pressure (95% CI 6.20–9.70), 0.030 for the right ventricular hypertrophy index (95% CI 0.010–0.050), 5.97 for medial wall thickness percentage (95% CI 3.12–11.70), and 12.00 for collagen volume fraction (95% CI 9.20–18.30).

Table 2. Pooled reference endpoints: SO versus RPAL ($n = 16$ per group), with the Hodges–Lehmann ligation-minus-sham difference.

Variable	Category	SO Median	RPAL Median	SO Mean ± SD	RPAL Mean ± SD	p	HL Difference	95% CI
RVSP (mmHg)	Hemodynamic	26.55	34.60	26.63 ± 0.88	34.42 ± 2.59	<0.001	8.05	6.20–9.70
RVHI	Pathology	0.28	0.31	0.278 ± 0.017	0.307 ± 0.032	0.006	0.030	0.010–0.050
%MT	Pathology	24.48	30.78	24.81 ± 1.17	32.03 ± 5.07	<0.001	5.97	3.12–11.70
CVF (%)	Pathology	6.50	16.75	6.01 ± 1.75	19.51 ± 5.73	<0.001	12.00	9.20–18.30

Medians and mean ± SD; two-sided Mann–Whitney U (pooled weeks 4–12). Differences are Hodges–Lehmann estimates with 95% confidence intervals corresponding to the two-sided Mann–Whitney U test. HL, Hodges–Lehmann; CI, confidence interval; SD, standard deviation.

3.3. Echocardiographic Predictors and Plasma LCN2 Level

At week 4, no echocardiographic index differed significantly between the groups (all $p \geq 0.05$; AT/ET $p = 0.056$; Table S3). Differences emerged mainly at weeks 8–12: at week 8, RVD1, RVWT, PAD, PAV, ET, and AT/ET differed between the groups (RVD1 $p = 0.004$; AT/ET $p = 0.044$), and at week 12, separation broadened further to include AT, TAPSE/(AT/ET), and TAPSE × AT, among other indices (Table S3). In the pooled analysis, the RPAL group showed higher RVD1, RVWT, PAD, ET, and TAPSE/(AT/ET), and lower TAPSE × AT, PAV, AT, and AT/ET (Table S4); RVD2, RVOTD, and TAPSE were nonsignificant. Plasma LCN2 level was higher in the RPAL group than in the SO group (13.66 vs. 6.06 ng/mL; $p < 0.001$). Thirteen of the 32 concentrations exceeded the stated assay range of 0.156–10 ng/mL and were not diluted: 12 after ligation and 1 after sham operation (maximum 32.443 ng/mL). The ligation median, 13.66 ng/mL, lies above that range.

At week 4, with five animals per group, the Hodges–Lehmann difference (ligation minus sham) was 4.15 ng/mL for plasma LCN2 (95% CI 2.01–6.46), 5.3 mmHg for right ventricular systolic pressure (3.3–7.4), 3.0 for medial wall thickness percentage (2.24–3.78), and 8.0 for collagen volume fraction (6.0–10.3). These intervals excluded zero. The echocardiographic differences had intervals that included zero: AT/ET, −0.046 (−0.074 to 0.007; $p = 0.056$); right ventricular diameter 1, 0.10 mm (−0.15 to 0.39); pulmonary artery diameter, −0.02 mm (−0.21 to 0.21); and pulmonary artery peak velocity, −0.08 m/s (−0.23 to 0.12).

Spearman correlations (Figure 2) showed LCN2 to be associated with RVSP ($\rho = 0.872$), RVHI ($\rho = 0.822$), %MT ($\rho = 0.895$), and CVF ($\rho = 0.837$) (all $p < 0.001$). Among echo indices, AT/ET ($\rho = -0.818$), PAV ($\rho = -0.808$), PAD ($\rho = 0.786$), and RVD1 ($\rho = 0.862$) correlated most strongly with RVSP; TAPSE/(AT/ET) correlated positively ($\rho = 0.707$), whereas TAPSE × AT correlated inversely ($\rho = -0.622$) with RVSP.

3.4. Primary Models and Partial Correlations

Primary LOOCV AUCs were 0.914 for M1 (bootstrap 95% CI 0.798–0.992) and 0.945 for M2 (0.847–1.000) (Table 3, Figure 3A). The increase in leave-one-out area under the curve was not statistically significant (ΔAUC +0.031; 95% CI 0.000–0.089; $p = 0.174$; Table 4). Integrated discrimination improvement was 0.061 (95% CI 0.031–0.095; $p < 0.001$) [22]. This improvement is not a significant gain in the area under the curve. Unpenalized M1 and M2 areas under the curve were 0.797 and 1.000; these two fits are not listed in Table 3. Full-panel ridge leave-one-out areas under the curve at C = 0.1 were 0.855 and 0.887 (Table 3).

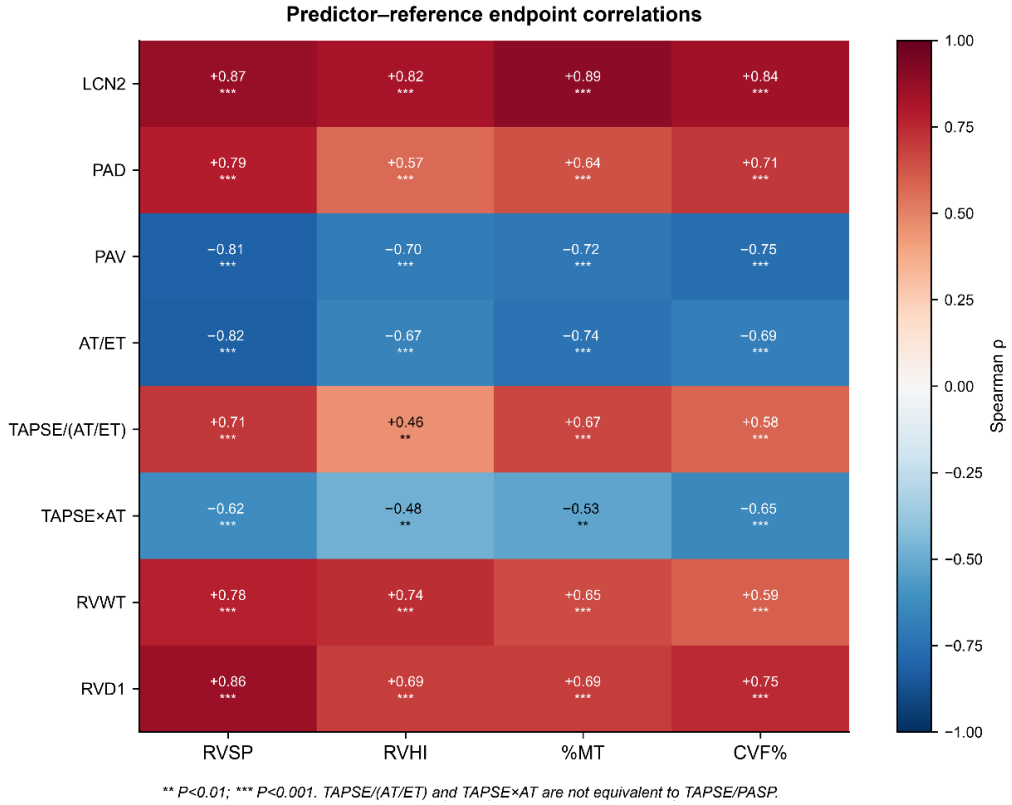


Figure 2. Spearman correlations between noninvasive predictors and reference endpoints ($n = 32$). Cell values are Spearman ρ. ** $p < 0.01$; *** $p < 0.001$, two-sided. TAPSE/(AT/ET) and TAPSE × AT are exploratory constructs and are not the ratio of TAPSE to pulmonary artery systolic pressure. AT, pulmonary artery acceleration time; CVF, collagen volume fraction; ET, pulmonary artery ejection time; LCN2, lipocalin-2; %MT, medial wall thickness percentage; PAD, pulmonary artery diameter; PAV, pulmonary artery peak velocity; RVHI, right ventricular hypertrophy index; RVD1, right ventricular diameter 1; RVSP, right ventricular systolic pressure; RVWT, right ventricular wall thickness; TAPSE, tricuspid annular plane systolic excursion.

Table 3. Three-track ridge-logistic discrimination for RPAL versus SO ($n = 32$).

Model	LOOCV AUC	Bootstrap 95% CI	Sens	Spec	Acc	Apparent AUC
M1 (primary)	0.914	0.798–0.992	0.750	1.000	0.875	0.973
M2 (primary)	0.945	0.847–1.000	0.812	1.000	0.906	0.992
E1 (secondary)	0.805	0.617–0.949	0.812	0.812	0.812	0.879
E2 (secondary)	0.961	0.882–1.000	1.000	0.875	0.938	1.000
E3 (secondary)	0.777	0.600–0.927	0.812	0.688	0.750	0.844
E4 (secondary)	0.988	0.951–1.000	0.938	1.000	0.969	1.000
Full panel, C = 0.1	0.855	0.699–0.973	0.688	1.000	0.844	—
Full panel + LCN2, C = 0.1	0.887	0.742–0.987	0.750	1.000	0.875	—

M1–M2 and E1–E4: ridge-logistic leave-one-out cross-validation at C = 1.0. Sensitivity rows: full-panel ridge-logistic leave-one-out cross-validation at C = 0.1. Bootstrap 95% CIs (B = 2000). Primary contrast M1 versus M2; E1–E4 exploratory; sensitivity rows are non-primary. Acc, accuracy; AUC, area under the curve; CI, confidence interval; LOOCV, leave-one-out cross-validation; Sens, sensitivity; Spec, specificity.

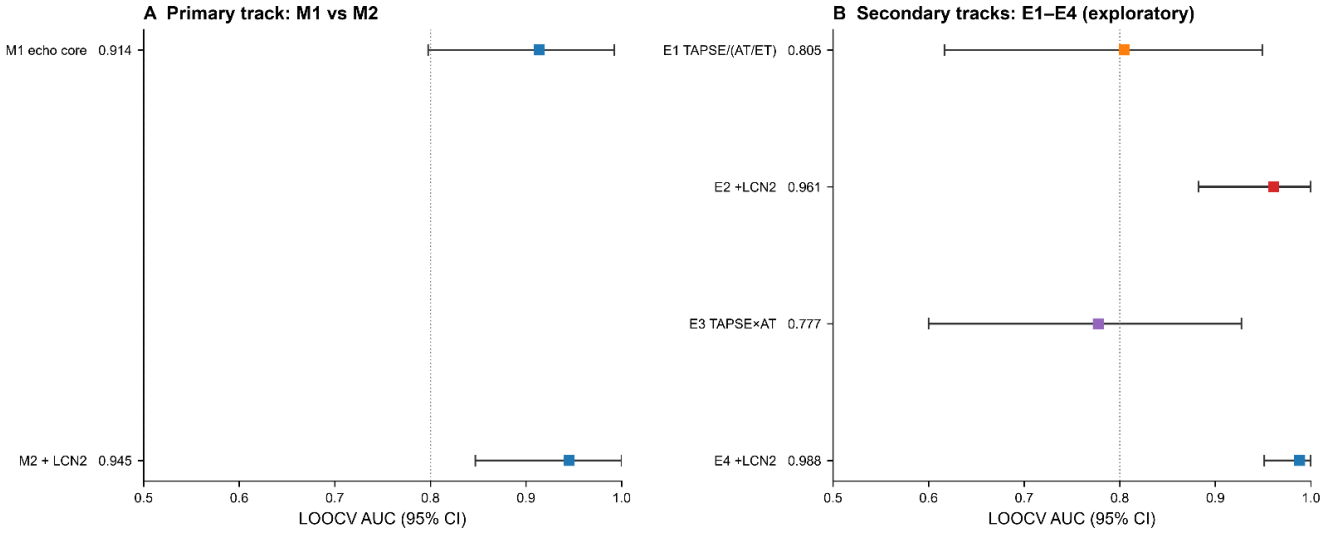


Figure 3. Leave-one-out cross-validated discrimination from ridge-logistic models (n = 32; penalty C = 1.0; standardization inside each training fold; bootstrap 95% confidence intervals from 2000 resamples). (**A**) Primary comparison. M1 contained right ventricular diameter 1, pulmonary artery diameter, pulmonary artery peak velocity, AT/ET, and postoperative week. M2 added plasma LCN2. The area under the curve increased from 0.914 to 0.945 (ΔAUC +0.031; 95% CI 0.000–0.089; p = 0.174). This increase was not statistically significant (two-sided $p < 0.05$ threshold). Integrated discrimination improvement was 0.061 (95% CI 0.031–0.095). Continuous prediction of right ventricular systolic pressure is reported in Section 3.6 and Figure 4. Leave-one-out R^2 increased from 0.819 to 0.847, and the in-sample nested change in R^2 was 0.028 (95% CI 0.0008–0.087; q = 0.004). (**B**) Exploratory single-construct tracks E1–E4. AT, pulmonary artery acceleration time; AUC, area under the curve; CI, confidence interval; ET, pulmonary artery ejection time; LCN2, lipocalin-2; LOOCV, leave-one-out cross-validation; TAPSE, tricuspid annular plane systolic excursion; the dotted vertical line marks an AUC of 0.8.

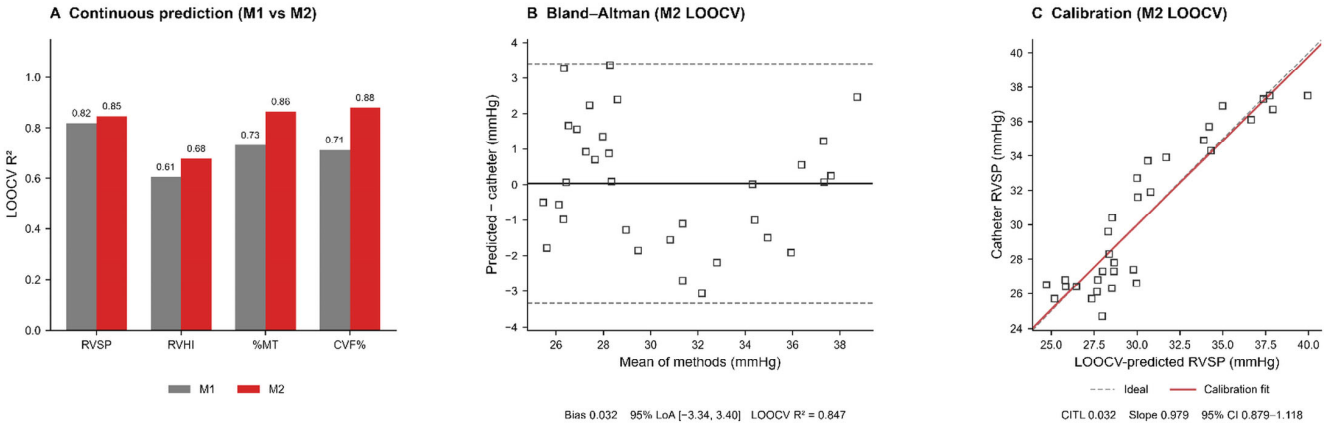


Figure 4. Continuous prediction of right ventricular systolic pressure, agreement, and calibration for the primary models (n = 32). (**A**) Leave-one-out cross-validated R^2 for right ventricular systolic pressure, the hypertrophy index, medial wall thickness percentage, and collagen volume fraction, for M1 and for M2 (M1 plus plasma LCN2). (**B**) Bland–Altman comparison of leave-one-out M2 predictions with catheter right ventricular systolic pressure (bias 0.032 mmHg; limits of agreement −3.34 to 3.40 mmHg). (**C**) Calibration of the M2 predictions (slope 0.979; bootstrap 95% CI 0.879–1.118). CITL, calibration-in-the-large; LoA, limits of agreement; LOOCV, leave-one-out cross-validation; M1, echocardiographic core plus postoperative week; CI, confidence interval.

Table 4. Bootstrap pairwise LOOCV AUC comparisons within the three-track framework.

Comparison	AUC Base	AUC New	ΔAUC	Bootstrap 95% CI	p (Bootstrap)
M1 vs. M2 (primary)	0.914	0.945	+0.031	0.000–0.089	0.174
E1 vs. E2 (secondary)	0.805	0.961	+0.156	0.032–0.302	0.021
E3 vs. E4 (secondary)	0.777	0.988	+0.211	0.071–0.375	0.006

Bootstrap ΔAUC from paired LOOCV probabilities (B = 2000).

After adjustment for postoperative week only, in all 32 animals, the Spearman partial correlations of LCN2 were 0.890 (95% CI 0.759–0.939) with right ventricular systolic pressure, 0.731 (0.450–0.894) with the right ventricular hypertrophy index, 0.868 (0.697–0.933) with medial wall thickness percentage, and 0.897 (0.780–0.941) with collagen volume fraction. No interval included zero. Relative to the unadjusted coefficients (0.872, 0.822, 0.895, and 0.837), the hypertrophy-index association was smaller. After adjustment for surgical group and postoperative week, the partial correlations were 0.285 (95% CI −0.049 to 0.598), 0.394 (−0.088 to 0.750), 0.050 (−0.361 to 0.516), and 0.438 (0.082–0.688). Only the collagen interval excluded zero. Within the 16 ligated animals, unadjusted Spearman correlations were 0.889 (95% CI 0.683–0.973), 0.923 (0.701–0.993), 0.826 (0.520–0.943), and 0.923 (0.735–0.979). After week was held constant, the partial correlations were 0.108 (95% CI −0.519 to 0.788), 0.597 (−0.152 to 0.973), −0.133 (−0.752 to 0.568), and 0.498 (−0.190 to 0.899). Every interval included zero. Within the 16 sham-operated animals, unadjusted Spearman correlations were 0.453 (95% CI −0.174 to 0.830) with right ventricular systolic pressure, 0.566 (0.060–0.888) with the right ventricular hypertrophy index, 0.677 (0.215–0.900) with medial wall thickness percentage, and 0.200 (−0.410 to 0.715) with collagen volume fraction. After week was held constant, the partial correlations were 0.358 (95% CI −0.147 to 0.807) with right ventricular systolic pressure, 0.171 (−0.457 to 0.744) with the right ventricular hypertrophy index, −0.032 (−0.634 to 0.764) with medial wall thickness percentage, and 0.534 (−0.048 to 0.892) with collagen volume fraction, and every interval included zero. In the ligated animals, adding LCN2 to week changed R^2 for right ventricular systolic pressure by 0.006 (coefficient 0.117 mmHg per ng/mL; 95% CI −0.245 to 0.479; $p = 0.49$). Adding LCN2 to a model that already contained group, week, and the group-by-week terms changed R^2 by 0.005 (coefficient 0.203 mmHg per ng/mL; 95% CI −0.034 to 0.439; $p = 0.090$). These coefficients, expressed per ng/mL, use the reported concentrations. Twelve of these concentrations after ligation and one after sham operation lie above the stated assay range (Section 3.3). Figure S1 identifies each animal by surgical group and postoperative week.

3.5. Secondary Exploratory Models (Tracks 2 and 3)

On the secondary tracks (E1 versus E2 and E3 versus E4), the leave-one-out area under the curve increased from 0.805 (95% CI 0.617–0.949) to 0.961 (0.882–1.000; ΔAUC +0.156; 95% CI 0.032–0.302; $p = 0.021$; integrated discrimination improvement 0.218) and from 0.777 (0.600–0.927) to 0.988 (0.951–1.000; ΔAUC +0.211; 95% CI 0.071–0.375; $p = 0.006$; integrated discrimination improvement 0.302), respectively (Tables 3 and 4, Figure 3B). These increments arise from weaker single-construct models, and TAPSE/(AT/ET) and TAPSE × AT are not TAPSE/PASP [18,19].

3.6. Continuous Prediction, Agreement, and Calibration

LOOCV RVSP R^2 increased from 0.819 (M1) to 0.847 (M2). The in-sample nested change in R^2 for right ventricular systolic pressure was 0.028 (likelihood-ratio $p = 0.004$; false-discovery-rate q = 0.004; Table S2, Figure S2). The bootstrap 95% confidence interval for this nested change, from 5000 resamples, was 0.0008–0.087. Secondary-track LOOCV R^2 increased from 0.568 to 0.764 (E1→E2) and from 0.372 to 0.791 (E3→E4) (Table S5). Bland–

Altman bias for LOOCV M2 was 0.032 mmHg (limits of agreement −3.34 to 3.40); calibration-in-the-large was 0.032 and calibration slope was 0.979 (bootstrap 95% CI 0.879–1.118) (Figure 4, Table S6) [23].

3.7. Exploratory, Internally Derived Cutoffs

Youden cutoffs (Table S7) are exploratory and specific to this model and assay. They are not clinically applicable thresholds and were not externally validated. They should not be equated with TAPSE/PASP indices. For example, LCN2 ≥ 9.69 ng/mL and AT/ET ≤ 0.466 yielded internal AUCs of 0.930 and 0.834, respectively (Table S7). The LCN2 point, 9.69 ng/mL, lies near the top of the stated calibration range, 0.156–10 ng/mL. Thirteen reported concentrations exceed that range and were not diluted, so the point is an internal description of this sample only.

4. Discussion

The principal findings of this study are as follows. First, isolated right pulmonary artery ligation produced the experimental volume-overload PH phenotype defined in the Introduction: higher catheter right ventricular systolic pressure than in sham-operated animals at weeks 4, 8, and 12, with higher medial wall thickness percentage and collagen volume fraction. Second, plasma LCN2 was associated with right ventricular systolic pressure and the histologic measures. Third, adding LCN2 improved integrated discrimination (0.061; 95% CI 0.031–0.095) and continuous prediction of right ventricular systolic pressure (leave-one-out R^2 0.819 to 0.847). The in-sample nested change in R^2 was 0.028 (95% CI 0.0008–0.087; q = 0.004). The leave-one-out area under the curve increased from 0.914 to 0.945 (ΔAUC +0.031; 95% CI 0.000–0.089; $p = 0.174$); that increase was not statistically significant. Secondary tracks showed larger increases in area under the curve from weaker single-construct baselines.

4.1. Validity of the Isolated RPAL Volume-Overload Phenotype

Once the right lung is excluded from perfusion, blood is redirected to the contralateral lung; total pulmonary blood flow does not increase, as it does with a left-to-right shunt. Left pulmonary arterial flow and cardiac output were not measured, so the extent of that redirection was not quantified. Even so, pooled across weeks 4–12, ligated animals showed higher right ventricular systolic pressure, right ventricular hypertrophy index, medial wall thickness percentage, and collagen volume fraction than sham-operated animals. The higher pressure can reflect the smaller perfused vascular bed as well as pulmonary arterial remodeling [24,25]. Higher left-lung medial thickness shows that pulmonary arterial remodeling occurred, and higher myocardial collagen indicates ventricular remodeling, but the data do not partition the pressure rise between those contributions. The ligation-only protocol matches the ligation arm of Meng et al. without a cervical systemic-to-pulmonary shunt [15]. In male rats, the phenotype over 12 weeks was early contralateral overcirculation, as expected when hyperperfusion occurs without hypoxia or chemical vasculopathy [4,5,15]. Irreversible pulmonary vascular disease was not demonstrated. Circulating LCN2 can be evaluated in this early phase, but whether the association persists once vascular disease becomes irreversible remains unresolved [5].

4.2. Echocardiographic Indices After Isolated Right Pulmonary Artery Ligation

At week 8, RVD1, RVWT, PAD, PAV, ET, and AT/ET differed between the ligated and sham-operated animals, and at week 12 the separation also included AT, TAPSE/(AT/ET), and TAPSE × AT, among other indices (Table S3). In the primary model, RVD1, PAD, PAV, AT/ET, and postoperative week already distinguished the two operations (leave-one-out

area under the curve 0.914). At week 4, when right ventricular systolic pressure, medial wall thickness percentage, collagen volume fraction, and plasma LCN2 were already higher after ligation, none of the echocardiographic indices differed significantly (all $p \geq 0.05$; AT/ET $p = 0.056$). Different animals were studied at each week, so this pattern does not show that echocardiography changed later within one animal, or that LCN2 detects pulmonary vascular disease earlier than echocardiography. Even in the pooled analyses, RVD2, RVOTD, and TAPSE did not differ significantly. Among these three, only TAPSE is used in a coupling ratio reported for patients. In patients with pulmonary arterial hypertension, the ratio of tricuspid annular plane systolic excursion to systolic pulmonary artery pressure has been studied as a noninvasive description of right ventricular–pulmonary arterial coupling [18,19,26]. TAPSE/(AT/ET) and TAPSE × AT, as calculated in the present model, are not that ratio, and clinical operating points reported for TAPSE/PASP are not used here. Neither construct differed significantly at week 4 or week 8, whereas both differed at week 12 (Table S3). TAPSE/(AT/ET) was higher after ligation largely because AT/ET declined, whereas raw TAPSE differed negligibly; TAPSE × AT declined in parallel with shortened acceleration time. Single-construct bases (E1 = TAPSE/(AT/ET) + week; E3 = TAPSE × AT + week) yielded modest leave-one-out areas under the curve (0.805 and 0.777). That modest separation is why the primary model combined several echocardiographic indices.

4.3. Association of Plasma LCN2 with Pressure and Histologic Measures

Plasma LCN2 showed strong Spearman associations with right ventricular systolic pressure ($\rho = 0.872$), the hypertrophy index ($\rho = 0.822$), medial wall thickness percentage ($\rho = 0.895$), and collagen volume fraction ($\rho = 0.837$). In other experiments, LCN2 has been linked to apoptosis resistance, phosphatidylinositol 3-kinase (PI3K)/Akt-dependent proliferation, and iron-facilitated endoplasmic reticulum stress in pulmonary arterial smooth-muscle cells [12–14]. Endoplasmic reticulum stress has also been examined in pulmonary hypertension apart from LCN2 [27]. Those pathways were not measured here. Because the LCN2 concentration rose without toxin exposure, the rise is not explained by chemical vasculopathy. Correlation does not establish causality: elevated LCN2 may reflect inflammation, endothelial or tissue injury, downstream remodeling, or more than one of these processes, and circulating LCN2 is not specific to the pulmonary vasculature [8].

The pooled correlations combine the ligation-versus-sham contrast with the differences across weeks 4, 8, and 12. Partial correlations adjusted for week only remained high (0.890, 0.731, 0.868, and 0.897) because that adjustment does not remove the group contrast. Removing that group contrast changes the result. After adjustment for surgical group and week, the partial correlation with right ventricular systolic pressure was 0.285 (95% CI −0.049 to 0.598); only the collagen interval among the four excluded zero. Within each operation, the pattern is the same: within ligated animals, and within sham-operated animals, the week-adjusted intervals included zero (Section 3.4). The collagen interval that excluded zero is not treated as evidence of residual severity, because its week-adjusted interval within the ligated animals included zero. These adjusted correlations do not show that LCN2 grades pressure once surgical group and week are taken into account. Seven days of hydrochlorothiazide were given after surgery, so an effect on circulating LCN2 cannot be excluded. Renal function, a systemic inflammatory panel, and LCN2 expression in pulmonary vascular tissue were not measured, so the source of the circulating concentration is uncertain. Reports of higher circulating LCN2 with higher pulmonary arterial pressure in congenital heart disease are directional context only [10,11].

4.4. Exploratory Primary and Secondary Models

To test whether LCN2 adds information beyond echocardiography, we used ridge-logistic leave-one-out cross-validation to compare an echocardiographic core with the same core plus LCN2. With 32 animals, a full ten-echo panel plus postoperative week is overparameterized, so the primary track kept only four echocardiographic indices plus postoperative week. Which four were kept was decided after inspecting their correlation with right ventricular systolic pressure in this same sample: RVD1, PAD, PAV, and AT/ET. That choice was not locked in an analysis plan before the inspection, and no optimism-corrected area under the curve is reported. The ridge penalty was fixed at C = 1.0. The negative coefficients for postoperative week in Table S1 are not interpreted as week effects. M1 already separated ligation from sham (area under the curve 0.914). Adding LCN2 raised it to 0.945, but that increase was not statistically significant (ΔAUC +0.031; 95% CI 0.000–0.089; $p = 0.174$). Integrated discrimination improved (0.061; 95% CI 0.031–0.095), as did continuous prediction of right ventricular systolic pressure (leave-one-out R^2 0.819 to 0.847). The in-sample nested change in R^2 was 0.028 (95% CI 0.0008–0.087; q = 0.004). Binary discrimination, integrated discrimination, and continuous regression address related but distinct questions [21,22]. At this sample size, precision for an increment of 0.03 is limited. The partial correlations in Section 4.3 fit this pattern: the association of LCN2 with right ventricular systolic pressure is carried largely by the contrast between ligation and sham, and the adjusted correlations do not show that LCN2 grades pressure once surgical group and week are taken into account. The sensitivity analyses do not replace this primary contrast. Unpenalized fits gave areas under the curve of 0.797 and 1.000, and full-panel ridge models at C = 0.1 gave leave-one-out areas under the curve of 0.855 and 0.887 (Table 3). The unpenalized fits are unstable, and the full-panel areas are lower than those of the primary core. On the secondary tracks, the area under the curve increased from 0.805 to 0.961 and from 0.777 to 0.988. Those larger increments start from weaker single-construct baselines, and the strong M1 baseline left little room for a further gain in the area under the curve.

4.5. Agreement Analysis: Cross-Validated Concordance Is Not Interchangeability

Leave-one-out predictions of catheter right ventricular systolic pressure from the model with LCN2 achieved $R^2 \approx 0.847$ with near-zero mean bias, yet Bland–Altman limits of agreement spanned approximately −3.34 to 3.40 mmHg [23]. Calibration-in-the-large was 0.032 and the calibration slope was 0.979 (bootstrap 95% CI 0.879–1.118 [21]). Acceptable calibration and a strong cross-validated R^2 describe agreement in this sample. Limits of agreement near ±3.4 mmHg may suit some research comparisons but would be wide for decisions that depend on a precise pressure threshold. Using leave-one-out predictions rather than apparent fitted values reduces optimism relative to in-sample agreement, and performance in a new cohort has not been tested.

4.6. Translational Implications for Pediatric CHD-PH Research

Timing of shunt repair and surveillance of early hyperperfusion remain central problems in pediatric congenital heart disease-associated pulmonary hypertension, for which serial right-heart catheterization is limited by anesthesia and resources [3–5]. The present results are not used to time an operation or to place a child on a surveillance pathway. The week-4 pattern in this male-rat ligation model, together with the gains in integrated discrimination and continuous prediction, identifies a preclinical question: whether a circulating marker adds information when early echocardiography does not separate the groups. The findings are tied to this experimental setting. Absolute rodent cutoffs, including the exploratory Youden points, are specific to this model and assay and are not applied to pediatric care [28]. Further use of the result would require an independent cohort [2,5].

4.7. Limitations

Certain limitations temper inference. First, isolated right pulmonary artery ligation does not reproduce an anatomic left-to-right shunt or increased total pulmonary blood flow [4,5,15]. Left pulmonary arterial flow and cardiac output were not measured, and irreversible pulmonary vascular disease was not demonstrated within 12 weeks. Second, 32 rats were analyzed, with 5–6 per group at each terminal week. No power calculation was performed for the incremental area under the curve, and animals were not added to offset deaths. Third, weeks 4, 8, and 12 used different animals. Fourth, hydrochlorothiazide was given for seven days after surgery and may have affected circulating LCN2. Injection logs, fluid balance, electrolytes, and renal function were not recorded. Fifth, the Youden cutoffs of 9.69 ng/mL for LCN2 and 0.466 for AT/ET are exploratory values from this sample and are not clinically applicable thresholds [28]. Sixth, mortality was 28.9% and higher after ligation, so survivor bias cannot be excluded (Table 1). Deaths included intraoperative, first-week, and terminal-procedure events, and the direction of bias cannot be determined. Seventh, no external cohort was studied. The echocardiographic predictors in M1 were chosen on the full sample, so no optimism-corrected area under the curve is reported. Eighth, TAPSE/(AT/ET) and TAPSE × AT are not TAPSE/PASP, and clinical TAPSE/PASP thresholds are not used here [18,19]. Ninth, the catheter remained in the right ventricle and was not advanced across the pulmonary valve, so pulmonary artery pressure, an outflow gradient, cardiac output, left-sided filling pressure, and pulmonary vascular resistance were not obtained. Right ventricular systolic pressure is the pressure-load endpoint. The right ventricular hypertrophy index is a structural endpoint and is not a hemodynamic measurement. Tenth, 13 of 32 LCN2 values exceeded the stated assay range of 0.156–10 ng/mL (12 after ligation and 1 after sham operation; maximum 32.443 ng/mL; ligation median 13.66 ng/mL); 50 µL undiluted of plasma was assayed; storage, freeze–thaw history, duplicates, and plate assignment were not recorded. Finally, the LCN2 associations do not establish causation, and circulating LCN2 is not specific to the pulmonary vasculature [8]. Accordingly, the present analyses remain hypothesis-generating.

5. Conclusions

Plasma LCN2 was higher after isolated right pulmonary artery ligation and was associated with catheter right ventricular systolic pressure and with histologic remodeling. The higher concentration was present at week 4, when the echocardiographic indices did not differ significantly. That result is between-group separation in different animals, not earlier detection within one animal. The primary models classify ligation against sham operation. They do not grade pulmonary hypertension. In the primary comparison, adding LCN2 did not significantly increase the leave-one-out area under the curve (ΔAUC +0.031; 95% CI 0.000–0.089; $p = 0.174$). The supported increments were in integrated discrimination (0.061; 95% CI 0.031–0.095) and in continuous prediction of right ventricular systolic pressure (leave-one-out R^2 0.819 to 0.847). The in-sample nested change in R^2 was 0.028 (95% CI 0.0008–0.087; q = 0.004).

Supplementary Materials: The following supporting information can be downloaded at https://www.mdpi.com/article/10.3390/jcdd13110573/s1: Figure S1: Plasma LCN2 against right ventricular systolic pressure, the right ventricular hypertrophy index, medial wall thickness percentage, and collagen volume fraction ($n = 32$); Figure S2: Incremental R^2 of adding plasma LCN2 to the primary echocardiographic core (M2 versus M1); Table S1: Standardized full-sample ridge-logistic coefficients; Table S2: Primary-track incremental value of LCN2 relative to M1; Table S3: Week-stratified Mann–Whitney comparisons of reference endpoints, LCN2, and the full echocardiographic panel (SO versus RPAL); Table S4: Pooled echocardiographic predictors and plasma LCN2: sham operation versus right pulmonary artery ligation ($n = 16$ per group); Table S5: Leave-one-out ridge regression performance

for continuous reference endpoints; Table S6: Bland–Altman agreement and calibration of leave-one-out M2 predictions versus catheter right ventricular systolic pressure; Table S7: Exploratory Youden points for classifying ligation versus sham in this sample. ARRIVE checklist file.

Author Contributions: Conceptualization, J.Y. and N.M.; methodology, J.Y.; software, L.X. (Li Xue) and L.X. (Liyuan Xu); validation, H.Z. and R.S.; formal analysis, Y.S.; investigation, J.Y.; resources, J.Y.; data curation, L.X. (Li Xue), L.X. (Liyuan Xu) and R.S.; writing—original draft preparation, J.Y.; writing—review and editing, N.M.; visualization, Y.S.; supervision, N.M.; project administration, N.M. and H.Z.; funding acquisition, J.Y. All authors have read and agreed to the published version of the manuscript.

Funding: This research was funded by the Natural Science Foundation of Beijing Municipality, grant number 7254349.

Institutional Review Board Statement: The animal study protocol was approved by the Institutional Animal Care and Use Committee of MDL Biotech (protocol code MDL2026-03-09-07; 9 March 2026).

Informed Consent Statement: Not applicable.

Data Availability Statement: The datasets generated and analyzed during the current study are available from the corresponding author on reasonable request. The analysis code is available from the corresponding author on request.

Conflicts of Interest: The authors declare no conflicts of interest. The funders had no role in the design of the study; in the collection, analyses, or interpretation of data; in the writing of the manuscript; or in the decision to publish the results.

Abbreviations

The following abbreviations are used in this manuscript:

%MT	medial wall thickness percentage
AT	pulmonary artery acceleration time
AUC	area under the curve
CHD-PH	pulmonary hypertension secondary to congenital heart disease
CI	confidence interval
CVF	collagen volume fraction
ED	external diameter
ELISA	enzyme-linked immunosorbent assay
ET	pulmonary artery ejection time
EVG	elastic–van Gieson
HL	Hodges–Lehmann
ID	internal diameter
LCN2	lipocalin-2
LOOCV	leave-one-out cross-validation
NGAL	neutrophil gelatinase-associated lipocalin
PAD	pulmonary artery diameter
PASP	pulmonary artery systolic pressure
PAV	pulmonary artery peak velocity
PBS	phosphate-buffered saline
PH	pulmonary hypertension
PI3K	phosphatidylinositol 3-kinase
RHC	right-heart catheterization
RPAL	right pulmonary artery ligation
RVD1	right ventricular diameter 1
RVD2	right ventricular diameter 2
RVHI	right ventricular hypertrophy index
RVOTD	right ventricular outflow tract diameter
RVSP	right ventricular systolic pressure
RVWT	right ventricular wall thickness
SO	sham operation
TAPSE	tricuspid annular plane systolic excursion
TR	tricuspid regurgitation

References

1. Simonneau, G.; Montani, D.; Celermajer, D.S.; Denton, C.P.; Gatzoulis, M.A.; Krowka, M.; Williams, P.G.; Souza, R. Haemodynamic definitions and updated clinical classification of pulmonary hypertension. *Eur. Respir. J.* **2019**, *53*, 1801913. [CrossRef]
2. Humbert, M.; Kovacs, G.; Hoeper, M.M.; Badagliacca, R.; Berger, R.M.F.; Brida, M.; Carlsen, J.; Coats, A.J.S.; Escribano-Subias, P.; Ferrari, P.; et al. 2022 ESC/ERS Guidelines for the diagnosis and treatment of pulmonary hypertension. *Eur. Heart J.* **2022**, *43*, 3618–3731. [CrossRef]
3. Abman, S.H.; Hansmann, G.; Archer, S.L.; Ivy, D.D.; Adatia, I.; Chung, W.K.; Hanna, B.D.; Rosenzweig, E.B.; Raj, J.U.; Cornfield, D.; et al. Pediatric pulmonary hypertension: Guidelines from the American Heart Association and American Thoracic Society. *Circulation* **2015**, *132*, 2037–2099. [CrossRef]
4. D'Alto, M.; Mahadevan, V.S. Pulmonary arterial hypertension associated with congenital heart disease. *Eur. Respir. Rev.* **2012**, *21*, 328–337. [CrossRef]
5. van der Feen, D.E.; Bartelds, B.; de Boer, R.A.; Berger, R.M.F. Pulmonary arterial hypertension in congenital heart disease: Translational opportunities to study the reversibility of pulmonary vascular disease. *Eur. Heart J.* **2017**, *38*, 2034–2041. [CrossRef]
6. Urboniene, D.; Haber, I.; Fang, Y.H.; Thenappan, T.; Archer, S.L. Validation of high-resolution echocardiography and magnetic resonance imaging vs. high-fidelity catheterization in experimental pulmonary hypertension. *Am. J. Physiol. Lung Cell. Mol. Physiol.* **2010**, *299*, L401–L412. [CrossRef]
7. Rudski, L.G.; Lai, W.W.; Afilalo, J.; Hua, L.; Handschumacher, M.D.; Chandrasekaran, K.; Solomon, S.D.; Louie, E.K.; Schiller, N.B. Guidelines for the echocardiographic assessment of the right heart in adults: A report from the American Society of Echocardiography endorsed by the European Association of Echocardiography, a registered branch of the European Society of Cardiology, and the Canadian Society of Echocardiography. *J. Am. Soc. Echocardiogr.* **2010**, *23*, 685–713. [CrossRef]
8. Chakraborty, S.; Kaur, S.; Guha, S.; Batra, S.K. The multifaceted roles of neutrophil gelatinase associated lipocalin (NGAL) in inflammation and cancer. *Biochim. Biophys. Acta* **2012**, *1826*, 129–169. [CrossRef]
9. Boucherat, O.; Vitry, G.; Trinh, I.; Paulin, R.; Provencher, S.; Bonnet, S. The cancer theory of pulmonary arterial hypertension. *Pulm. Circ.* **2017**, *7*, 285–299. [CrossRef]
10. Zhang, H.; Sun, T.; Yang, J.; Sun, Y.; Liu, G.; Krittanawong, C.; El-Am, E.A.; Bou Chaaya, R.G.; Xu, L.; Ye, Z.; et al. Lipocalin 2: Could it be a new biomarker in pediatric pulmonary hypertension associated with congenital heart disease? *Rev. Cardiovasc. Med.* **2021**, *22*, 531–536. [CrossRef]
11. Guo, Z.K.; Chen, P.G.; Li, Y.X.; Jiao, H.; Kong, X.H.; Bai, S.; Li, X.F.; Liu, A.J.; Wang, G.L. Independent prognostic value of lipocalin-2 in congenital heart disease-associated pulmonary artery hypertension. *World J. Cardiol.* **2024**, *16*, 720–730. [CrossRef]
12. Wang, G.; Liu, X.; Meng, L.; Liu, S.; Wang, L.; Li, J.; Cui, C.; Meng, J.; Hu, S.; Wei, Y. Up-regulated Lipocalin-2 in pulmonary hypertension involving in pulmonary artery SMC resistance to apoptosis. *Int. J. Biol. Sci.* **2014**, *10*, 798–806. [CrossRef]
13. Wang, G.; Ma, N.; Meng, L.; Wei, Y.; Gui, J. Activation of the phosphatidylinositol 3-kinase/Akt pathway is involved in lipocalin-2-promoted human pulmonary artery smooth muscle cell proliferation. *Mol. Cell Biochem.* **2015**, *410*, 207–213. [CrossRef]
14. Wang, G.; Liu, S.; Wang, L.; Meng, L.; Cui, C.; Zhang, H.; Hu, S.; Ma, N.; Wei, Y. Lipocalin-2 promotes endoplasmic reticulum stress and proliferation by augmenting intracellular iron in human pulmonary arterial smooth muscle cells. *Int. J. Biol. Sci.* **2017**, *13*, 135–144. [CrossRef]
15. Meng, L.; Liu, X.; Zheng, Z.; Li, J.; Meng, J.; Wei, Y.; Hu, S. Original rat model of high kinetic unilateral pulmonary hypertension surgically induced by combined surgery. *J. Thorac. Cardiovasc. Surg.* **2013**, *146*, 1220–1226.e1. [CrossRef]
16. National Research Council. *Guide for the Care and Use of Laboratory Animals*, 8th ed.; National Academies Press: Washington, DC, USA, 2011.
17. Percie du Sert, N.; Hurst, V.; Ahluwalia, A.; Alam, S.; Avey, M.T.; Baker, M.; Browne, W.J.; Clark, A.; Cuthill, I.C.; Dirnagl, U.; et al. The ARRIVE guidelines 2.0: Updated guidelines for reporting animal research. *PLoS Biol.* **2020**, *18*, e3000410. [CrossRef]
18. Guazzi, M.; Bandera, F.; Pelissero, G.; Castelvecchio, S.; Menicanti, L.; Ghio, S.; Temporelli, P.L.; Arena, R. Tricuspid annular plane systolic excursion and pulmonary arterial systolic pressure relationship in heart failure: An index of right ventricular contractile function and prognosis. *Am. J. Physiol. Heart Circ. Physiol.* **2013**, *305*, H1373–H1381. [CrossRef]
19. Tello, K.; Wan, J.; Dalmer, A.; Vanderpool, R.; Ghofrani, H.A.; Naeije, R.; Roller, F.; Mohajerani, E.; Seeger, W.; Herberg, U.; et al. Validation of the tricuspid annular plane systolic excursion/systolic pulmonary artery pressure ratio for the assessment of right ventricular-arterial coupling in severe pulmonary hypertension. *Circ. Cardiovasc. Imaging* **2019**, *12*, e009047. [CrossRef]
20. Fulton, R.M.; Hutchinson, E.C.; Jones, A.M. Ventricular weight in cardiac hypertrophy. *Br. Heart J.* **1952**, *14*, 413–420. [CrossRef]
21. Efron, B.; Tibshirani, R.J. *An Introduction to the Bootstrap*; Chapman & Hall: New York, NY, USA, 1993.
22. Pencina, M.J.; D'Agostino, R.B., Sr.; D'Agostino, R.B., Jr.; Vasan, R.S. Evaluating the added predictive ability of a new marker: From area under the ROC curve to reclassification and beyond. *Stat. Med.* **2008**, *27*, 157–172; discussion 207. [CrossRef]
23. Bland, J.M.; Altman, D.G. Statistical methods for assessing agreement between two methods of clinical measurement. *Lancet* **1986**, *1*, 307–310. [CrossRef]
24. Rabinovitch, M. Molecular pathogenesis of pulmonary arterial hypertension. *J. Clin. Invest.* **2012**, *122*, 4306–4313. [CrossRef]

25. Heath, D.; Edwards, J.E. The pathology of hypertensive pulmonary vascular disease; a description of six grades of structural changes in the pulmonary arteries with special reference to congenital cardiac septal defects. *Circulation* **1958**, *18*, 533–547. [CrossRef]
26. Chen, W.; Luo, X.; Luo, J.; Song, J.; Qiu, H.; Chen, J.; Fan, C.; Li, J. Clinical relevance of the TAPSE/SPAP ratio in pulmonary arterial hypertension: A single-center retrospective study. *BMC Cardiovasc. Disord.* **2026**, *26*, 190. [CrossRef]
27. Dromparis, P.; Paulin, R.; Stenson, T.H.; Haromy, A.; Sutendra, G.; Michelakis, E.D. Attenuating endoplasmic reticulum stress as a novel therapeutic strategy in pulmonary hypertension. *Circulation* **2013**, *127*, 115–125. [CrossRef]
28. Youden, W.J. Index for rating diagnostic tests. *Cancer* **1950**, *3*, 32–35. [CrossRef]

Disclaimer/Publisher's Note: The statements, opinions and data contained in all publications are solely those of the individual author(s) and contributor(s) and not of MDPI and/or the editor(s). MDPI and/or the editor(s) disclaim responsibility for any injury to people or property resulting from any ideas, methods, instructions or products referred to in the content.